energies

Article

Study on Artificial Filter Cake Evaluation Method of Oleophilic Nano-Plugging Agent

Feng Dai [1,2], Pingya Luo [1,*], Chunlin Wu [2], Rui Wang [3], Yingmin Liu [2] and Weian Huang [3]

1 School of Petroleum Engineering, Southwest Petroleum University, Chengdu 610500, China
2 Exploration and Development Department, Sichuan Changning Natural Gas Development Co., Ltd., Chengdu 610051, China
3 School of Petroleum Engineering, China University of Petroleum (East China), Qingdao 266580, China
* Correspondence: luopy@swpu.edu.cn

Abstract: Oil-based drilling fluid is currently widely utilized when drilling shale, in which the oleophilic nano-plugging agent is the major component for wellbore strengthening. However, there have been few effective and straightforward evaluation methods for the nano-plugging agent. In this study, an artificial filter cake was created to simulate the microfissure of shale formation, and the performance of the nano-plugging agent was assessed using the fluid-loss reduction rate as the index. The filter cake was made from compound crystal weights and a high molecular weight polymer, and a nano-plugging agent matching the formation pore structures was selected. The performance of three plugging agents with varying particle sizes (ultrafine $CaCO_3$, emulsified modified rubber MORLF, ULIA nano-plugging agent) was compared. Moreover, the validity of the evaluation process was confirmed, and the underlying plugging mechanism was investigated. The proposed technique can produce an artificial filter cake with a constant thickness of 3×10^{-3} m and a permeability in the range of 10^{-18} to 10^{-19} m^2, and the assessment approach is consistent, precise and easy to use. This work may provide a guideline for evaluating oleophilic nano-plugging agents in the laboratory and field applications.

Keywords: oleophilic nano-plugging agent; wellbore stability; sealing evaluation; artificial filter cake; complex barite

Citation: Dai, F.; Luo, P.; Wu, C.; Wang, R.; Liu, Y.; Huang, W. Study on Artificial Filter Cake Evaluation Method of Oleophilic Nano-Plugging Agent. *Energies* **2023**, *16*, 3559. https://doi.org/10.3390/en16083559

Academic Editor: Rouhi Farajzadeh

Received: 12 March 2023
Revised: 4 April 2023
Accepted: 12 April 2023
Published: 20 April 2023

1. Introduction

There are many micro-fractures and pores in shale gas formations, which are prone to shaft wall instability in the drilling process. Shaft wall collapse, diameter reduction, drilling fluid leakage, reservoir pollution and other complex downhole conditions caused by shaft wall instability will delay the drilling cycle, increase the drilling cost, and may also affect the following steps such as cementing and oil recovery [1].

In the study of borehole stability, the factors that affect borehole stability usually include hydration and pressure transfer. The drilling fluid systems used for horizontal well drilling of shale gas mainly use an oil-based drilling fluid, which helps to stabilize shale walls and solves the problem of high friction. However, the problems of hole collapse and sticking are more prominent in the drilling process, and fracture leakage occurs sometimes. There are nanoscale fractures and pores in hard and brittle shale. If these structures can be sealed to prevent liquid entry and reduce the influence of various factors on shale formation, the problem of wellbore instability will be solved. Conventional drilling fluid plugging agents use materials with particle sizes that are too large. It is thus difficult for them to enter the nanometer scale pores in mud shale, to form a dense plugging layer. Nano-micron materials have high surface activity, uneven particle surface, and easy adsorption by other substances. Nano-particles are very small, which enables them to fill and plug micro-cracks and pores in mud shale, and to seal mud shale tightly [2–4].

At present, there is no unified standard for evaluating nano-plugging agents. There are several different methods for evaluating the plugging effect of nano-plugging agents and drilling fluid systems. Thus, Yue Qiansheng et al. [5] used a low permeability artificial core, a slicing metal core and the filter cake permeability of oil-based drilling fluid to characterize the micro-fracture plugging ability of a single treatment agent and drilling fluid system in order to simulate the micro-fractures of hard brittle shale.

According to the characteristics of micro-fractured strata, Chen Liang [6] used a self-made metal seam plate in combination with a high temperature and high pressure static water loss instrument. Adjusted by the ruler and screw, the iron block could simulate a micro-crack of 20–100 µm; the depth of the micro-crack was 5 mm, the internal surface of the crack was rough, and the internal crack could be observed after the experiment, which was simple and practical. The simulation effect of microcracks was accurate.

Yang Juqian et al. [7] used dry drilling to obtain the standard core column, made cracks on the core column, simulated micro-cracks of different widths (micron level) by using tinfoil of different thicknesses on the core joint surface, put the set core column into the core holder, and used the dynamic water loss instrument to evaluate the plugging ability of mudstone micro-cracks.

Yan Jing [8] used natural core and metal foil and cementing material of different thicknesses to pour into micro-cracks designed to simulate the real pore-throat and micro-cracks. Combined with the outer cylinder of the high-temperature and high-pressure water loss instrument and the mud cup, the leakage amount within 30 min was monitored and the plugging performance of the plugging agent was evaluated. The simulated core had a minimum crack width of 3.33 µm, a stroke of 5–10 cm, and a high repetition rate.

The pore pressure transfer test device can carry out hydraulic pressure difference transfer testing of mud shale and can measure the permeability of very low mud shale. A permeability pressure transfer test induced by chemical potential difference can also be carried out to measure the efficiency of shale film. Since the bulk elastic modulus of water is very large and water is almost incompressible, pressure can be quickly built up in a closed cavity filled with water when there are slight changes in the geometric volume of the cavity. Using the characteristics of a semi-permeable membrane, the relationship between drilling fluid, borehole wall (semi-permeable membrane) and formation fluid can be simulated in real drilling processes when the initial pressure difference between the two ends of a shale core is not zero. The pressure relationship (actual pressure difference) measured in real time by the pore pressure transfer evaluation device directly reflects the pressure change relationship on both sides of the semi-permeable film; the fluid migration situation on both sides of the semi-permeable film (well wall) can be analyzed and judged, providing an intuitive rating for treatment agent evaluation and effective guidance for drilling fluid performance design [9].

These methods are all direct simulations of rock fractures, and have a certain guiding role in evaluating the plugging effect of nano-plugging agents and drilling fluid [10], but they have problems such as poor repeatability and inability to conduct in-depth analysis and study of the mechanism of plugging from a microscopic perspective [11–14]. To address this limitation, the present study improved the existing experimental methods. It used nano-barite and ordinary barite compounded with enhanced molecular polymer to prepare artificial filter cake as the filter medium, then simulated the formation micro-cracks and pores, and selected a nano-plugging agent matching the formation, thereby realizing the organic combination of intuitive and quantitative research [15,16].

2. Evaluation Method

The plugging evaluation experimental method using a sand pan can evaluate the performance of a plugging agent under the simulated condition of a downhole high temperature and high pressure environment [17]. However, as a filtration medium, the sand pan is expensive and cannot be reused; a low permeability sand pan is difficult to obtain, and it cannot fully simulate the pore structure of a low permeability formation.

In terms of mud cake, the filling and packing effect of heavy stone particles with different particle sizes is different, and this directly affects the quality of the mud cake [18]. Reasonable particle size matching leads to a higher degree of mud cake density. The density of mud cake has a great influence on its porosity, permeability, strength, filtration, thickness, smoothness, etc. Mud cakes with high density packing have low porosity, low permeability, high strength, small thickness and low fluid loss, which is reflected in the mud cake quality. In order to improve the quality of mud cake, the combination of different particle sizes was studied to find the best mixing method using heavy stone. By improving the existing experimental methods, an artificial filter cake was prepared with nano-barite and ordinary barite combined with a high molecular polymer as the filter medium [19–21]. The diameter of common barite used alone is too large, the size distribution range is small, and the permeability of the mud cake formed is high. When barite with different sizes is mixed, the permeability of the mud cake is much lower than that of single barite mud cake. In each group, when the ratio of 0.89 μm barite to common barite was 4:10, the highest packing density and the best cake quality were obtained. The artificial mud cake simulates the formation's micro-cracks and pores, and enables selection of the nano-plugging agent matching the formation. The permeability of shale in the target formation is stable in the range of 10^{-18}–10^{-19} m^2, which realizes the organic combination of intuitive and quantitative research.

2.1. Experimental Setup

The high temperature and pressure filtration meter is shown in Figure 1, which consists of a pressure source (either CO_2 or N_2), a pressure regulator, a drilling fluid cup with a pressure bearing capacity of 4140–8690 kPa, a fitting bracket, an oil-resistant seal, an end cap that supports the filter medium, and a valve stem above the filtrate discharge tube for controlling filtrate release [22].

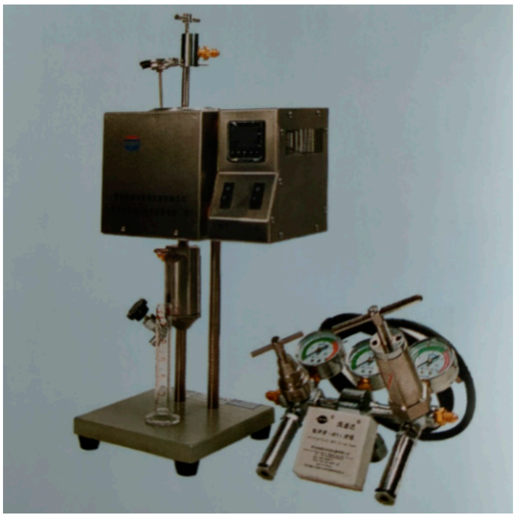

Figure 1. High temperature and pressure filtration instrument.

The sample was prepared by mixing a portion of the filter cake base slurry, stirring for half an hour, and putting it in the drilling fluid cup. Then a high-pressure filtration loss test was carried out at ambient temperature/3.45×10^6 Pa as per the standard procedure in GB/T 16783.1-2014. After the measurement, the drilling fluid was removed from the cup. The inner wall of the cup was washed slowly with distilled water to wash away excessive test slurry on the surface of the filter cake and the clean filter cake was obtained.

After adding 100 mL of distilled water to the drilling fluid cup with the filter cake inside, the filtration loss was measured at 3.45×10^6 Pa and room temperature for 30 min. The result was noted as L_1.

The experimental steps are as follows. Measure 20.0 g (accurately to 0.01 g) of plugging agent sample and place it into a beaker with 180 mL of distilled water or white oil, and agitate the mixture with an ultrasonic disperser for 15 min before setting it aside.

Remove the drilling fluid cup, open the unfiltered end, discard the distilled water, add 100 mL of the specified sample solution to the drilling fluid cup, agitate with a glass rod, put the drilling fluid cup back together, and measure the filtration loss at ambient temperature and 3.45×10^6 Pa for 30 min, and record the result as L_2. If $L_2 \geq L_1$, investigate the reason and remake the filter cake; otherwise, move on to the next assessment.

The sample solution is substituted with distilled water, and the decrease in permeability filtration of pure water after blocking is noted as L_3.

The permeability reduction rate can be obtained from Equation (1):

$$P = \frac{L_1 - L_3}{L_1} \times 100\% \tag{1}$$

where P is the permeability reduction rate, %; L_1 is the filter loss of clean water before plugging, mL; L_3 is the filter loss of clean water after plugging, measured in milliliters, mL.

2.2. Optimized Cake Assay Formulation

Firstly, the formula of ordinary barite-based slurry was tested. 400 mL distilled water was measured using a 500 mL cylinder and put into a mixing cup. Under the condition of high-speed agitation (load speed (11,000 ± 300) r/min), bentonite (measured to 0.01 g) and 0.6 g anhydrous sodium carbonate (measured to 0.01 g) for slurry preparation of drilling fluid were added. Further steps were as follows. Stir for 20 min and pause at least twice during the period to scrape off the bentonite attached to the container wall. Place the prepared test slurry at (25 ± 3) °C for closed curing for 24 h. Slowly add 120.0 g barite powder that has been dried to constant weight at (105 ± 3) °C (measured to 0.01 g) at high-speed agitation (load speed (11,000 ± 300) r/min), and stir for 30 min. The filtrate loss is measured at 105 °C and 3.5×10^6 Pa by the high temperature and high pressure filtrate loss instrument. Then the drilling fluid inside the instrument is poured out, a small amount of distilled water is injected into the inner wall of the instrument, and the water is poured out after gentle shaking. Then the distilled water is injected to the scale, and the filtration loss of mud cake under distilled water condition is measured at 105 °C and 3.5×10^6 Pa, and the reading is recorded for 30 min. Take out the mud cake from the instrument, use the hot fan to bake and blow the mud cake for 20 s, and then use the needle in the meter to measure its thickness. The average permeability K of mud cake can be calculated as follows:

$$K = \frac{q \cdot l \cdot \mu}{A \cdot \triangle p} \tag{2}$$

where K is the average permeability of filter cake, $\times 10^{-12}$ m^2; q is distilled water filtration loss volume per unit time, $\times 10^{-6}$ m^3/s; l is the thickness of filter cake, $\times 10^{-2}$ m; μ is the viscosity of distilled water under experimental conditions, $\times 10^{-3}$ Pa·s; A is filter cake area, $\times 10^{-4}$ m^2; $\triangle p$ is experimental differential pressure, 10^6 Pa.

The viscosity of distilled water μ at 25 °C is 0.8937×10^{-3} Pa·s. The measured cake area A is 23.8×10^{-4} m^2, and the experimental pressure difference $\triangle p$ is 3.5×10^6 Pa.

The permeability of ordinary barite-based slurry artificial mud cake is shown in Table 1. The water loss is too high, and the average permeability is 2×10^{-18} m^2, which is higher than the required standard. The formula of mud-cake-based slurry needs to be improved.

An artificial core needs to be manufactured, which can simulate the cracks and pores. By blending ordinary barite (200 µm) and nanometer barite (0.89 µm) into a polymer solution, dispersing it into a homogenous suspension, and then compressing it into a fixed-sized filter cake through the application of high pressure, it is possible to replicate nano and nano-micron pores of a formation, and thus, use the cake as a reproducible artificial core simulation.

Table 1. Experimental results of common barite-based slurry artificial mud cake.

Experiment Serial Number	Cake Making		Clearwater Test		Cake Thickness /10^{-3} m	Permeability /10^{-18} m^2 Time/h
	Time/h	Water Loss/mL	Time/s	Water Loss/mL		
1	2	30	1800	11.6	3	2.07
2	2	31	1800	11.4	3	2.04
3	2	33	1800	13.5	3	2.41
4	2	32.5	1800	13.0	3	2.32

Experiments (1# to 4# in Table 2) were prepared by mixing 100 g of nano-barite with 1000 mL of water, 0.3% polyacrylamide, and 0.9% sodium polyacrylate, in the ratios of 200 µm: 0.89 µm = 10:1, 10:2, 10:3, 10:4, respectively. The filter cake was created after two hours of being pressurized at 3.5×10^6 Pa and evaluated by submerging it in clean water for 30 min at 3.5×10^6 Pa. After removing the filter cake from the apparatus, it was heated with a hot air fan for 20 s and its thickness measured with an acupuncture meter. The findings are shown in Table 2 and Figure 2, for different barite conditions.

Table 2. Performance of filter cake under different compound barite conditions.

Experiment Serial Number	Cake Making		Clearwater Test		Cake Thickness /10^{-3} m	Permeability /10^{-18} m^2
	Time/h	Water Loss/mL	Time/s	Water Loss/mL		
1#	2	90	1800	28.5	17.20	30.723
2#	2	22	1800	2.9	8.82	1.605
3#	2	25	1800	3.2	5.40	1.085
4#	2	19	1800	2.4	3.24	0.429

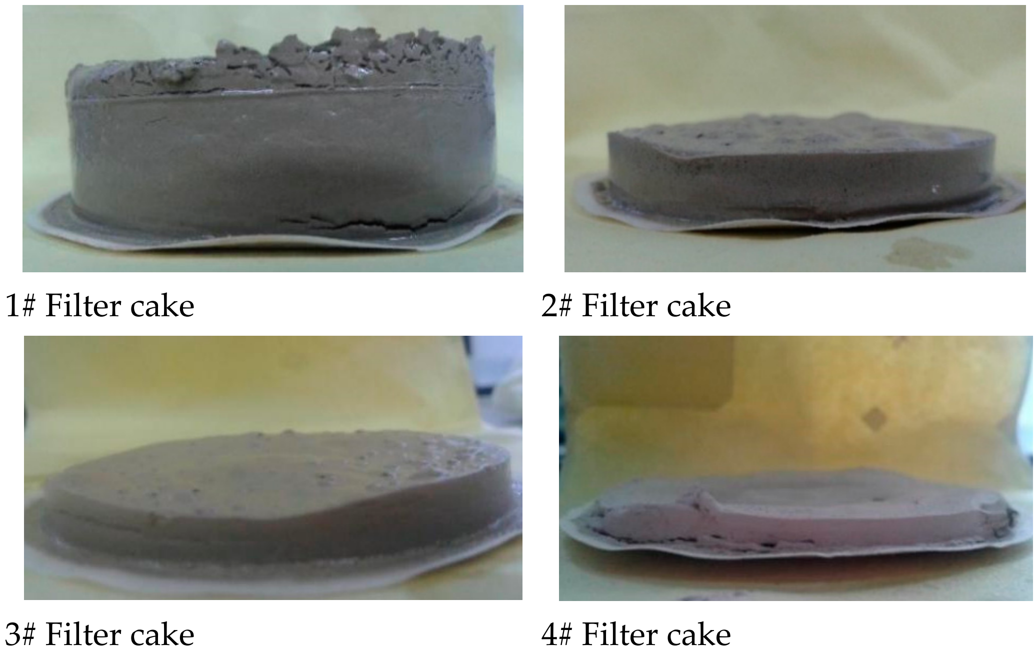

Figure 2. Filter cake diagram under different compound barite conditions.

Next, the ratio of viscosifier polyacrylamide to sodium polyacrylate in the mud cake base paste was varied, and the experimental results are shown in Table 3.

Table 3. Experimental results for synthetic clay cake with composite barite base slurry.

Polyacrylamide/%	Sodium Polyacrylate/%	Cake Making		Clearwater Test		Cake Thickness /10^{-3} m	Permeability /10^{-18} m^2
		Time/h	Water Loss/mL	Time/s	Water Loss/mL		
0.3	0.3	2	60	1800	14.0	9	0.0498
0.3	0.8	2	19	1800	2.0	3	1.0465
0.3	0.9	2	20	1800	2.2	3	0.9514
0.3	1.0	2	25	1800	4.0	2	0.7849

Based on the experimental results, the formula for the nano-blocking simulation of "artificial core" using experiment 4# was determined, and the process for its manufacture was established as following steps:

- Add 0.3% polyacrylamide and 0.9% sodium polyacrylate to 1000 mL of water and stir for 1 h to dissolve completely.
- Add 100 g of nano-barite and 250 g of ordinary barite while stirring, and stir at high speed for 15~20 min to make it fully and evenly mixed.
- Pour into the GGS71 high temperature and pressure dehydration meter scale line (about 200 mL), filter at room temperature, 3.5×10^6 Pa, and prepare the filter cake after two hours of water loss.
- Open the instrument, fill it with clean water, and measure the permeability of the filter cake at a pressure of 3.5×10^6 Pa, which is 10^{-18}–10^{-19} m^2 as qualified.

3. Accuracy and Parallelism Analysis of Evaluation Methods

3.1. Parallelism Analysis

Ten trials of parallel experiments were conducted to assess the permeability and thickness of the artificial filter cake, the outcomes of which are presented in Table 4. The water loss of the clean water test was consistent at 2~2.5 mL, the thickness of the artificial filter cake was roughly 3×10^{-3} m, and its permeability was in the range of 10^{-18} to 10^{-19} m^2. The results show minimal variation, indicating that the artificial filter cake produced by this method exhibits excellent parallelism and stability.

Table 4. Parallelism experiment of artificial filter cake.

Experiment Serial Number	Cake Making		Clearwater Test		Cake Thickness /10^{-3} m	Permeability /10^{-18} m^2
	Time/h	Water Loss/mL	Time/s	Water Loss/mL		
1	2	17.5	1800	2.5	3.12	0.447
2	2	18	1800	2.4	3.20	0.429
3	2	15	1800	2.2	2.96	0.393
4	2	18	1800	2.5	2.98	0.447
5	2	17.5	1800	2.4	2.95	0.429
6	2	18.5	1800	2.2	3.05	0.393
7	2	21	1800	2.4	3.01	0.429
8	2	17	1800	2.2	2.97	0.393
9	2	24.5	1800	2.4	3.05	0.429
10	2	25.5	1800	2.0	2.89	0.358

3.2. Accuracy Analysis

For this research, three nano-plugging agents with significant variations in particle size were selected to test the precision of the assessment procedures, including ultrafine $CaCO_3$, emulsified rubber MORLF, and ULIA nano-plugging agents. The intermediate diameters of ultrafine $CaCO_3$, emulsified rubber MORLF, and ULIA nano-plugging agents are 38,150 nm, 584 nm, and 2442 nm.

Figure 3 shows that the emulsion-modified rubber MORLF with the smallest average particle size had the highest permeability loss reduction rate and the best-plugging performance compared with the other two plugging agents. Figure 4 illustrates that the filter cake with emulsified modified rubber MORLF plugging is much more consistent than the other two, resulting in a black waxy sealing layer on the cake's surface. In contrast, there is not much difference in the macroscopic appearance of the cake before and after ultrafine calcium carbonate and ULIA nano-plugging agent sealing. This experimental technique is able to accurately assess the effectiveness of a nano-plugging agent so that the particle size and shape of the plugging agent can be precisely adjusted to fit the microcracks and pores for successful sealing.

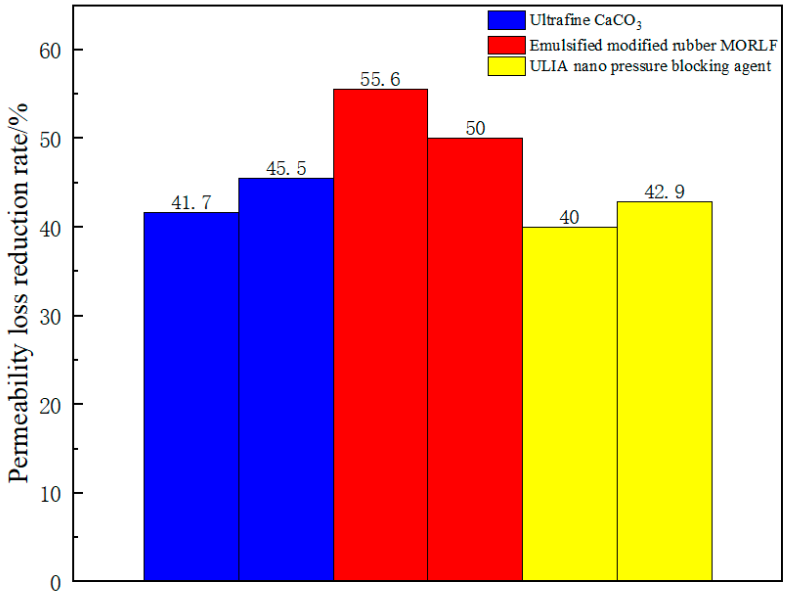

Figure 3. Results of artificial filter cake permeability filtration loss reduction rate test.

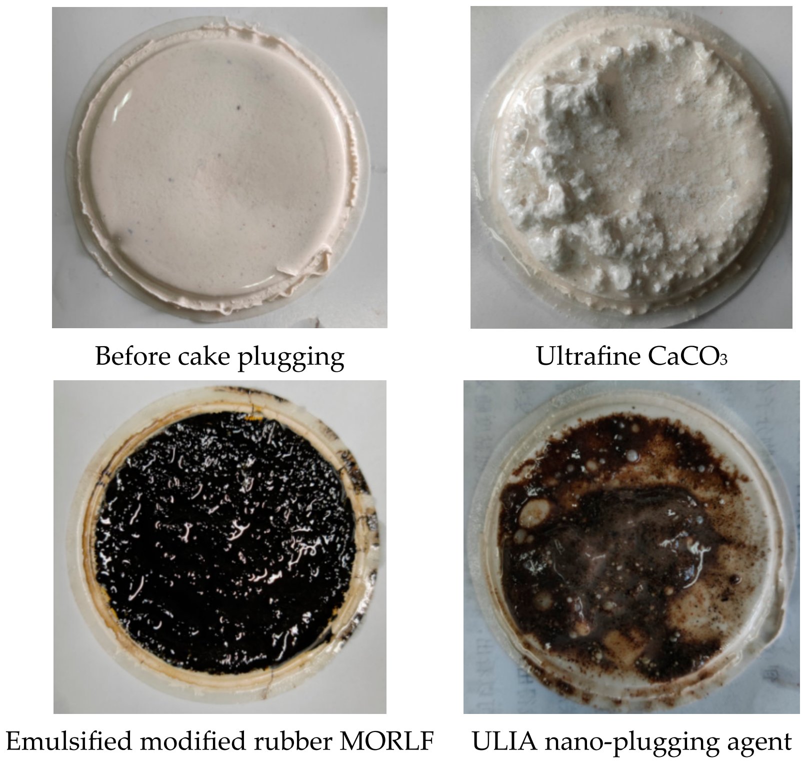

Figure 4. Comparison chart of filter cake before and after plugging.

4. Field Application

4.1. Application Overview

The application of the nano-plugging agent identified through the above experiment has been successful in the Changning region, thus resolving the horizontal section of the target formation's wellbore stability problems. The utilization of nano-plugging agents in the wells of this region resulted in an average 9.74% decrease in hole diameter enlargement rate and an average 5.4-day reduction in the drilling and completion period, in comparison to the values obtained when the agent was not used during drilling in complex formations.

Water-based drilling fluid is used in the first to third section of well Ning 209H42-1, and oil-based drilling fluid is used in the fourth section. In order to ensure that oil-based drilling fluid can successfully replace water-based drilling fluid in the middle of the third section, water is used to displace water-based drilling fluid in the casing sections in advance, and a large flow rate is used to fully cycle the cleaning of the casing, so as to ensure a balanced density of water in the inlet and outlet. In order to reduce the mixing zone, the displacement rate is high and the displacement time is fixed. During the cycle, wetting agent and emulsifier should be added in time to keep the performance of the drilling fluid system stable.

4.2. Typical Well Example

4.2.1. Overview and Drilling Fluid Difficulties

The Ning 209H42-1 well (shown in Figure 5) is situated in the southern portion of the Zhongaoding Structure of Changning Anticline Structure at the fringe of the Sichuan Basin, with an intended ending depth of 4497 m and a final depth of 4350 m. This well is a shale gas horizontal well in Southwest Oilfield, and its main target is Longmaxi Formation. According to the actual drilling data of the adjacent well, shale fractures have developed in the Longmaxi Formation in this block, which facilitates leakage, and complex situations such as collapse and sticking occur easily in the drilling process. Therefore, the content of plugging agent in the oil-based drilling fluid system should be increased. The measured formation pressure value after drilling and fracturing in this area is abnormally high, and there may be abnormal high pressure if drilling into the fracture zone.

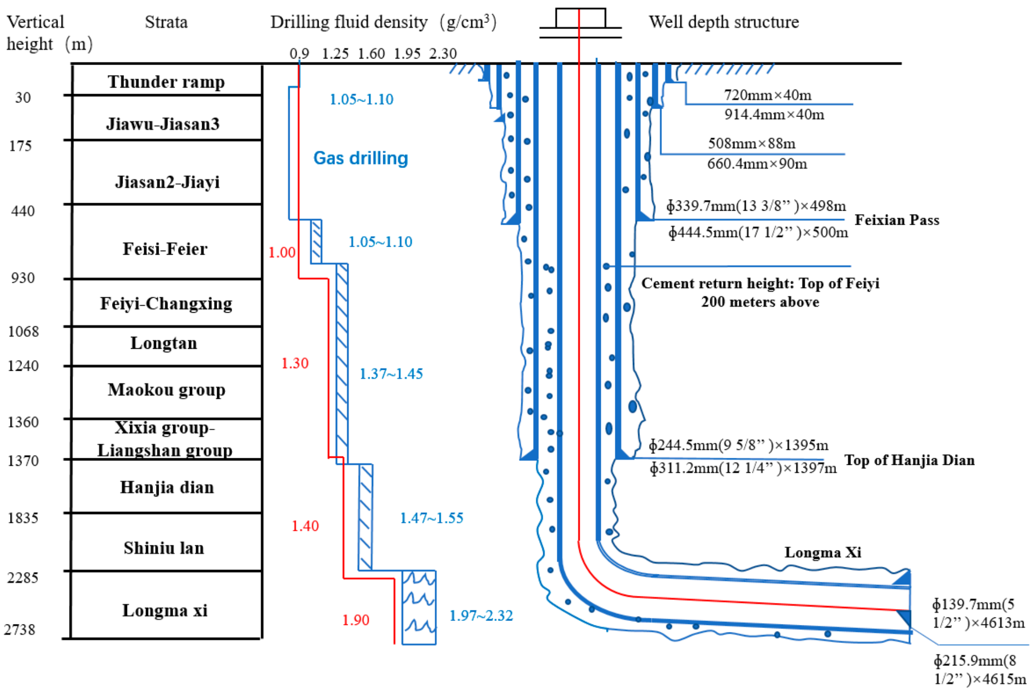

Figure 5. Chart of casing program of Well Ning209H42-1.

4.2.2. In Situ Application Effects

The whole well was filled with nano-plugging drilling fluid bored to a depth of 1748 m. The nano-plugging drilling fluid is regularly checked during the drilling process and the oil-water ratio is regulated to the range 85~90/15~10 before entering the inclination point, with the demulsification voltage kept at around 1300 V and the high temperature and pressure filtration loss kept to below 2 mL. The study demonstrates that the nano-plugging drilling fluid is user-friendly in practical scenarios, allowing for easy adjustment of rheology and filtration loss, thus decreasing the risk of downhole failure. The nano-plugging agent displays excellent prevention properties and is highly resistant to collapse, and there are no complex issues such as well wall spalling or block loss during construction.

The filtration loss was used as the evaluation criterion to compare the plugging performance of nano-micron drilling fluid and adjacent oil-based drilling fluid in Binning 209H42-1 well. The average 30 min filtration loss of Ning 209H42-2 well, Ning 209H42-4 well, Ning 209H50-2 well, Ning 209H50-4 well and Ning 209H42-1 well was 12 mL, 10 mL, 8 mL, 9 mL and 2 mL, respectively. Results show that the 30 min filtration loss of nano-plugging drilling fluid used in Ning 209H42-1 well was the smallest, and the plugging ability was the strongest. Hence, the nano-plugging agent selected can reduce the wellbore instability on-site.

5. Conclusions

When the particle size is uniform or the particle size range is very narrow, the filling effect of small particles on large particles is not obvious, and the packing density is low. On the contrary, when there are multiple particle size segments, the filling effect of small particles on large particles is obvious during the accumulation of solid particles, and the mud cake formed has a high packing density. Low particle packing density leads to high porosity of the mud cake, and high porosity leads to high permeability and high filtration loss. Meanwhile, the internal structure strength of mud cake with high porosity is low. Therefore, the quality of clay cake obtained by barite using a single grain size composition is obviously worse than that obtained by compound particle weight mixtures.

When mixed in different ways, the particle size difference of small particles is different, the filling effect of small particles on large particles is different, and the packing density of mud cake will also be different. When the radius of the small particles is equal to the radius of the crystal hole, the filling effect of the small particles on the crystal hole is the best, with the highest packing density and achieving the ideal filling effect. When the radius of the small particles is larger than the radius of the crystal pore, the small particles will produce an outward "support force" on the structure formed by the large particles, resulting in lattice destruction and reduced packing density. When the radius of small particles is small, small particles easily "leak" from the crystal pore and cannot stay in place. However, relative to the radius of the crystal pore, the radius of small particles is generally not too small, so the "leakage" phenomenon of small particles in the crystal pore is less; the packing density will be reduced relative to the ideal filling density, but not too much.

The combination of barite particles in various sizes yields a much more effective filter cake than simply using barite alone. When a ratio of 4:10 barite size is blended, the filter cake has the highest density and optimal quality. The thickness of the manufactured filter cake was maintained at 3×10^{-3} m, while the permeability remained steady in the range 10^{-18}–10^{-19} m^2 under 3.45×10^6 Pa for 2 h. The filter cake, which is artificially created, can be used to replicate the micro-fractures that form naturally, and the nano-plugging agent which is appropriate for the formation's pore structure can be chosen exactly. The test results demonstrate a high degree of precision and excellent consistency.

Evaluation methods for nano-plugging agents can be further studied. In future studies, artificial mud cake can be developed by optimizing the formula of artificial mud cake, so as to evaluate the plugging agents of different sizes, and to further develop the evaluation method of plugging agents under simulations of different formation conditions.

Author Contributions: Conceptualization, F.D.; Methodology, P.L.; Validation, P.L.; Formal analysis, C.W.; Investigation, F.D. and R.W.; Writing—original draft, F.D.; Writing—review & editing, P.L.; Visualization, W.H.; Funding acquisition, C.W. and Y.L. All authors have read and agreed to the published version of the manuscript.

Funding: This work was financially supported by the Key Science and Technology Research Project of Sichuan Changning Natural Gas Development Co., Ltd. (Project No.: 20210604-12).

Data Availability Statement: The data that support the findings of this study are available from the corresponding author upon reasonable request.

Acknowledgments: The authors thank Ming Lei for the data analysis and document arrangement.

Conflicts of Interest: The authors have no conflict to disclose.

References

1. Liu, J.; Sun, J. Mechanism and inhibition method of wellbore hydration instability in shale gas reservoir. *Drill. Complet. Fluids* **2016**, *33*, 5.
2. Wang, X.; Bai, D.; Sun, Y.; Li, C.; Lu, Z.; Jing, Y.; Liu, C.; Jiang, L. Enhanced plugging of all oil-based drilling fluid system for shale gas wells—*Take* Weiyuan Block in Changning Weiyuan National Shale Gas Demonstration Area as an example. *Nat. Gas Ind.* **2020**, *12*, 1–5+20.
3. Chen, X.; Tan, C.P.; Detournay, C. A study on wellbore stability in fractured rock masses with impact of mud infiltration. *J. Petrol. Sci. Eng.* **2003**, *38*, 145–154. [CrossRef]
4. Huang, W.; Qiu, Z.; Xu, J.; Yu, L. Experimental study on wellbore instability mechanism in Western Tuha Oilfield. *J. Pet.* **2007**, *28*.
5. Yue, Q.; Li, Y.; He, B.; Li, Z.; Xiang, X.; Wang, J.; Li, Y. Research on hard and brittle shale in Weizhou 12-1N Oilfield and technical countermeasures for drilling fluid. *China Offshore Oil Gas* **2005**, *17*, 44–47.
6. Chen, L. *Research on Evaluation Method and Plugging Mechanism of Drilling Fluid Anti Collapse Plugging*; Southwest Petroleum University: Chengdu, China, 2013.
7. Yang, F.A.; Hou, J. A new method for shale micro fracture simulation and plugging evaluation experiment. *Drill. Complet. Fluids* **2017**, *34*, 45–49.
8. Yan, J. Simulation and simulation plugging experiment of micro fracture core for plugging evaluation. *Prospect. Eng. (Geotech. Drill. Eng.)* **2018**, *45*, 18–21.
9. Wang, J.; Yan, J.; Su, S. A new method for wellbore stability evaluation of hard brittle shale. *Pet. Drill. Prod. Technol.* **2006**, 28–30+83. [CrossRef]
10. Ma, H.; Zhang, H.; Zhang, Y. Well bore stability analysis based on THM. *J. Daqing Pet. Inst.* **2008**, *32*, 50–55.
11. Huang, R.Z.; Chen, M.; Deng, J.G.; Wang, K.P.; Chen, Z.X. Study on shale stability of wellbore by mechanics coupling with chemistry method. *Drill. Fluid Complet. Fluid* **1995**, *12*, 15–22.
12. Qiu, Z.S.; Xu, J.F.; Lv, K.H.; Yu, L.X.; Wang, Z.M. A multivariate cooperation principle for well-bore stabilization. *Acta Pet. Sin.* **2007**, *28*, 117–119.
13. Li, W.; Wang, P.; Wang, B.; Luo, P.; Yang, K.; Pu, L. After satisfying the asteroid impact on the quality of water-based drilling fluid filter cake. *J. Chongqing Inst. Technol.* **2014**, *4*, 69–72.
14. Hu, Y.; Yue, Q.; Liu, S.; Chen, L. Research on the soft shale drilling fluid in BZ29-4S oilfield. *J. OilGas Technol.* **2012**, *34*, 94–97.
15. Qiu, Z.; Li, J.; Shen, Z. New method for water sensitivity evaluation of shale—A study on specific water wettability. *Oil Drill. Prod. Technol.* **1999**, *21*, 1–6.
16. Qiu, Z.; Ding, R.; Yu, L. The determining method researching of specific surface area for mud shale. *Drill. Fluid Complet. Fluid* **1999**, *16*, 9–11.
17. Cai, J.; Chenevert, M.E.; Sharma, M.M.; Friedheim, J.E. Decreasing Water Invasion into Atoka Shale Using Nonmodified Silica Nanoparticles. *SPE Drill. Complet.* **2012**, *27*, 103–112. [CrossRef]
18. Hoelscher, K.P.; De Stefano, G.; Riley, M.; Young, S. Application of Nanotechnology in Drilling Fluids. In Proceedings of the SPE International Oilfield Nanotechnology Conference and Exhibition, Noordwijk, The Netherlands, 12–14 June 2012. SPE 135642.
19. Sensoy, T.; Chenevert, M.E.; Sharma, M.M. Minimizing Water Invasion in Shale Using Nanoparticles. In Proceedings of the SPE Annual Technical Conference and Exhibition, New Orleans, LA, USA, 4–7 October 2009. SPE 124429.
20. Al-Bazali, T.M.; Zhang, J.; Sharma, M.M. Measurement of the Sealing Capacity of Shale Caprocks. In Proceedings of the SPE Annual Technical Conference and Exhibition, Dallas, TX, USA, 9–12 October 2005. SPE 59632.

21. Cao, X.C.; Qin, Y.; Zhao, Y.N.; Ke, K. Basic Performance Research of Polymer Intercalation Clay. *Adv. Mater. Res.* **2012**, *578*, 183–186. [CrossRef]
22. Srivatsa, J.T.; Ziaja, M.B. An Experimental Investigation on Use of Nanoparticles as Fluid Loss Additives in a Surfactant-Polymer Based Drilling Fluid. In Proceedings of the International Petroleum Technology Conference, Bangkok, Thailand, 7–9 February 2012.